

# HI line observations of luminous infrared galaxy mergers

W. van Driel<sup>1,2</sup>, Yu Gao<sup>3</sup>, D. Monnier-Ragaine<sup>1,2</sup>

<sup>1</sup> Unité Scientifique Nançay, USR CNRS B704, Observatoire de Paris, 5 place Jules Janssen, F-92195 Meudon, France

<sup>2</sup> DAEC, UMR CNRS 8631, Observatoire de Paris, 5 place Jules Janssen, F-92195 Meudon, France

<sup>3</sup> IPAC, Caltech, MS 100-22, 770 South Wilson Ave., Pasadena, CA 91125, U.S.A.

Received 22/9/2000; accepted 22/12/2000

**Abstract.** A total of 19 luminous infrared galaxy mergers, with  $L_{\text{IR}} \gtrsim 2 \times 10^{11} L_{\odot}$ , for  $H_0 = 75 \text{ km s}^{-1} \text{ Mpc}^{-1}$ , have been observed in the HI line at Nançay and four of them were observed at Arecibo as well. Of these 19, ten had not been observed before. Six were clearly detected, one of which for the first time. The objective was to statistically sample the HI gas mass in luminous infrared mergers along a starburst merger sequence where the molecular CO gas content is already known. We also searched the literature for HI data and compared these with our observations.

**Key words:** Galaxies: distances and redshifts – Galaxies: general – Galaxies: ISM – Radio lines: galaxies

## 1. Introduction

Most luminous infrared galaxies (LIGs), with infrared luminosities  $L_{\text{IR}} \gtrsim 2 \times 10^{11} L_{\odot}$ , for  $H_0 = 75 \text{ km s}^{-1} \text{ Mpc}^{-1}$ , are gas-rich, closely interacting/merging systems (e.g., van den Broek et al. 1991; Sanders 1992; Murphy et al. 1996) with high star formation rates and efficiencies. They represent the dominant population among objects with  $L_{\text{bol}} \gtrsim 2 \times 10^{11} L_{\odot}$  in the local universe (Sanders & Mirabel 1996).

Most of the LIGs' luminosity is radiated by dust in the far-infrared. Evidence in favor of a starburst origin for the high IR luminosity is clearly mounting (e.g., from molecular gas content, Downes & Solomon 1998; Solomon et al. 1997; radio continuum imaging, Condon et al. 1991; Smith et al. 1998; ISO mid-IR spectroscopy, Genzel et al. 1998; and ground based mid-IR and HST/NICMOS near-IR imaging, Soifer et al. 2000; Scoville et al. 2000). Although an AGN might also contribute to the high IR luminosity of a small fraction LIGs (e.g., Sanders et al. 1988; Veilleux et al. 1997; 1999; Sanders 1999), the observed abundant supply of *dense* molecular gas traced by high dipole moment molecules like HCN, usually found

only in star formation cores (Solomon et al. 1992; Gao 1996; Gao & Solomon 2000a, b) indicates that almost all LIGs are ideal stellar nurseries.

A clear correlation between the CO(1-0) luminosity (a measure of molecular gas mass  $M(\text{H}_2)$ ) and the projected separation of merger nuclei (an indicator of merging stages) has been shown for a sample of 50 LIG mergers (Gao & Solomon 1999), indicating that the molecular gas content decreases as merging advances. This suggests that the molecular gas content is being rapidly depleted due to the starbursts as merging progresses. This was the first evidence connecting the depletion of molecular gas with starbursts in interacting galaxies. The question arises if a similar relationship exists between the HI gas mass and the merger interaction stages.

Only loose correlations were found between the HI gas mass and  $L_{\text{IR}}$  in previous HI line studies of LIGs samples of LIGs (Garwood et al. 1987; Jackson et al. 1989; Martin et al. 1991; Mirabel & Sanders 1988; Young et al. 1986), unlike the tight correlation found between  $L_{\text{IR}}$  and the CO gas mass. A tighter correlation was found (Kennicutt 1998) between the  $L_{\text{FIR}}/\text{area}$  and  $M_{\text{HI}}/\text{area}$ , however. This may imply that the more diffuse HI gas is being depleted as well, like the molecular gas component, as merging advances.

The  $M(\text{H}_2)/M(\text{H I})$  ratio also increases with  $L_{\text{IR}}$  for LIGs (Mirabel & Sanders 1989). However, whether this ratio increases or not as the merging progresses through different stages has not yet been explored. With new HI data accumulated for a statistically significant sample of LIGs arranged along a starburst merger sequence (e.g., by the degree of nuclear separation and the merging morphology compared with numerical simulations for mergers), we can ultimately examine how the  $M(\text{H}_2)/M(\text{H I})$  ratio changes as the merger-induced starburst proceeds in mergers of different stages, since the molecular gas contents of our sample galaxies are already known.

Just over a dozen galaxies in the Gao & Solomon (1999) CO sample of LIG mergers have 21cm HI line measurements reported in the literature. In order to enlarge the sample available for a statistical study of the relationship between the HI gas mass and the evolution of the

merging process as the starburst proceeds along a starburst merger sequence, we have conducted new HI observations. Here, we present the results of new Nançay and Arecibo 21cm observations of 19 LIGs in the sample (for the sample selection, see Sect. 2).

We will explore possible correlations with the global HI properties of LIGs in detail in another paper (Gao et al. in preparation). For this, we will use all HI observations available for LIGs in the CO survey of Gao & Solomon (1999), including spectra from an unpublished Arecibo HI survey of LIGs (I.F. Mirabel 1997, private communication).

## 2. Sample selection – luminous infrared galaxies along a starburst merger sequence

Although there have been extensive HI and CO observations of LIGs, including synthesis imaging (e.g., Mirabel & Sanders 1988; Martin et al. 1991; Scoville et al. 1991; Gao 1996; Gao et al. 1997; Lo, Gao & Gruendl 1997; Downes & Solomon 1998; Hibbard & Yun 1996, 1999a, 1999b; Gao & Solomon 1999; Gao et al. 1999, 2000a, b), there has been no systematic attempt to trace the gas properties (both atomic and molecular) during the galaxy-galaxy merger sequence starting with systems roughly separated by a galactic diameter; e.g., just 4 galaxies in the “Toomre Sequence” (Toomre & Toomre 1972; Toomre 1977), representing a merger sequence, were observed by Hibbard & van Gorkom (1996).

However, observations of only the atomic gas along the “Toomre Sequence” is not sufficient to trace the starburst processes occurring during a galaxy-galaxy merger, as stars are forming in molecular clouds which are probably embedded in the more diffuse atomic hydrogen gas, and HI itself is not a tracer of the star forming gas. Moreover, the galaxy mergers in the “Toomre Sequence” are optically selected and have large variations in their gas content and do not easily fit into a sequence of gas conversion into stars.

Although the “Toomre Sequence” nicely reflects the dynamical transformation of two spiral galaxies into a merged elliptical, no ultraluminous starburst is included in this sequence – the four most infrared luminous objects on the sequence are NGC 6621/2, NGC 7592, NGC 2623 and NGC 3256, with, respectively,  $\log(L_{IR}/L_{\odot})=11.26, 11.33, 11.55$  and  $11.57$ . Therefore, although the triggering of a starburst by the merging of two spiral galaxies is probably represented by the “Toomre Sequence”, it poorly samples the ultraluminous starburst phase of gas-rich mergers along the merger sequence. In short, the “Toomre Sequence” is most likely a morphological sequence, and it tells us little about the conversion of gas into stars during mergers. Indeed, there are many close mergers where the progenitors are not gas-rich galaxies and these may never become LIGs (e.g., Bushouse et al. 1988; Kennicutt et al. 1987).

The ideal sample to trace a merger sequence leading to the formation of an ultraluminous starburst would contain gas-rich galaxies of various merging stages that initially started with roughly comparably, large gas contents. Since this is impossible to ascertain, we selected LIGs where the 2 progenitors can be identified from CCD images. By measuring the HI content as a function of the merger separation for a sample with known molecular gas properties, the time dependence of the total (HI+CO) gas properties can then be traced statistically in a starburst merger sequence.

50 LIGs with  $L_{IR} \gtrsim 2 \times 10^{11} L_{\odot}$ ,  $2'' \lesssim S_{sep} \lesssim (D_1 + D_2)/2$  (where  $S_{sep}$  is the separation between nuclei and  $D_1$  and  $D_2$  are the major axis diameters of the two galaxies) have been selected for the CO study of Gao & Solomon (1999), and we already have molecular gas measurements for all these galaxies. Here, we aim at establishing a large homogeneous sample of LIGs which have HI measurements as well. For observation at Nançay, we excluded all high redshift ( $cz > 20,000 \text{ km s}^{-1}$ ) sources, deemed *a priori* too weak in HI for a 100m-class telescope, and all southern sky ( $\delta < -39^\circ$ ) objects inaccessible from the site, thus reducing the sample to 30 LIGs. By further excluding sources around the Galactic Center’s right ascension, where the transit telescope is too heavily oversubscribed with high-priority targets, and by avoiding the repetition of previously well-detected sources, we ended up with a total sample of 19 LIGs from our CO sample (see Table 1). For all of these we obtained new global HI spectra.

## 3. Observations and data reduction

### 3.1. Nançay observations

The Nançay telescope is a meridian transit-type instrument of the Kraus/Ohio State design, consisting of a fixed spherical mirror, 300 m long and 35 m high, a tiltable flat mirror (200×40 m), and a focal carriage moving along a 90 m long curved rail track, which allows the tracking of a source on the celestial equator for about 1 hour. Located in the centre of France, it can reach declinations as low as  $-39^\circ$ . It has an effective collecting area of about 7000 m<sup>2</sup> (equivalent to a 94-m diameter parabolic dish). Due to the elongated mirror geometry, at 21-cm wavelength it has a half-power beam width of 3'6 E-W×22' N-S for declinations below  $20^\circ$ , increasing to 34' N-S at  $\delta=65^\circ$ , the highest declination in the present survey (E. Gérard, private comm.; see also Matthews & van Driel 2000). Typical system temperatures were  $\sim 40$  K for our project.

Our observations were made throughout the period December 1998 - October 1999, using a total of about 150 hours of telescope time. We obtained our observations in total power (position-switching) mode using consecutive pairs of two-minute on- and two-minute off-source integrations. Off-source integrations were taken at approximately  $2''$  E of the target position. The autocorrelator was divided into two pairs of cross-polarized receiver banks, each

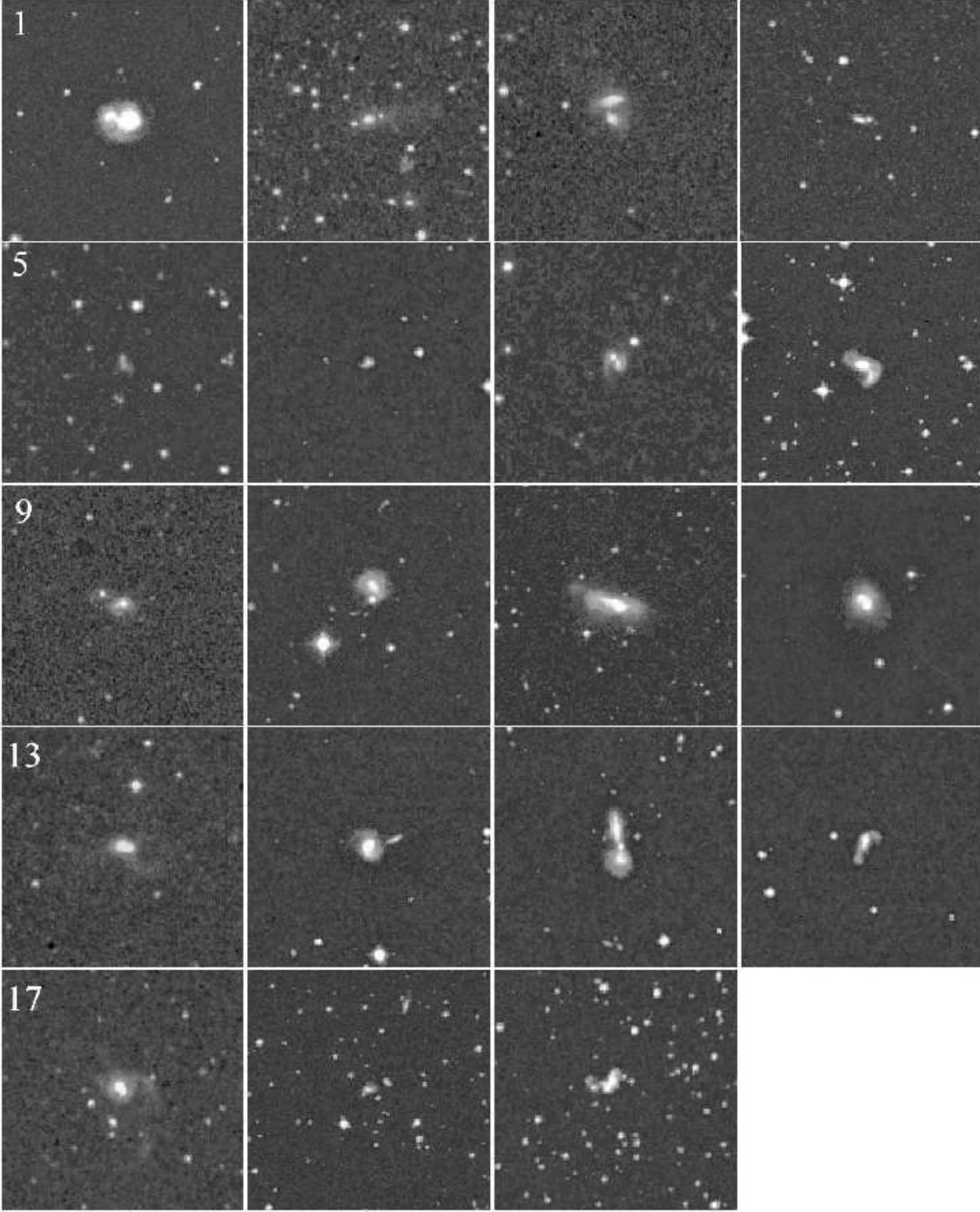


**Fig. 1.** Mosaic of Digital Sky Survey images of the 19 infrared luminous merger galaxies observed. The dimensions of the individual images are  $5' \times 5'$ . The order of the galaxies is the same as that used in the Tables.

with 512 channels and a 6.4 MHz bandpass. This yielded a channel spacing of  $2.64 \text{ km s}^{-1}$  and an effective velocity resolution of  $\sim 3.3 \text{ km s}^{-1}$ , which was smoothed to a channel separation of 13.2 and a velocity resolution of  $15.8 \text{ km s}^{-1}$  during the data reduction, in order to search for faint features. The centre frequencies of the two banks

were set to the known redshifted H I frequency of the target; all galaxies had existing optical and CO redshifts.

We reduced our H I spectra using the standard DAC and SIR spectral line reduction packages available at the Nançay site. With this software we subtracted baselines (generally third order polynomials) and averaged the two receiver polarizations. To convert from units of  $T_{sys}$  to

**Table 1.** Basic optical data for the sample galaxies.

No.	Ident	R.A.			Dec			$V_{opt}$	err	$B_T$	D×d	Morph	Spect	sep
		(1950.0)												
		hh	mm	ss.s	dd	mm	ss	km/s	km/s	mag	' × '			"
1	IC 1623A	01 05	19.9		-17 46	29		6042	72	13.70	1.0 0.8	Sp:	H II	16.0
	IC 1623B	01 05	22.0		-17 46	18		5840	60	15.00	0.8 0.6		H II	
2	IRAS 02483+4302	02 48	19.8		43 02	53		15475	105	16.75	0.6 0.3			3.8
3	UGC 2369A	02 51	15.9		14 46	24		9463	152	15.39	0.7 0.3	Sb		22.5
	UGC 2369B	02 51	15.9		14 46	03		9380	118	15.54	0.7 0.4			
4	IRAS 03359+1523	03 35	57.5		15 23	10		10626	45	16.58	0.4 0.2		H II	10.0
5	IRAS 04232+1436	04 23	15.2		14 36	53		23972	60	18.60	0.3 0.2			4.6
6	IRAS 08572+3915	08 57	12.9		39 15	39		17480	42	(14.92)			L:/Sy2	5.5
7	IRAS 10035+4852	10 03	35.7		48 52	23		19396	50	16.13	0.6 0.4			8.7
8	IC 2545	10 03	53.0		-33 38	30		10245	47	15.25	0.65 0.4			5.0
		10 03	52.0		-33 38	42				(16.83)				
9	IRAS 10565+2448W	10 56	35.5		24 48	43	(13160)	(81)						8.0
	IRAS 10565+2448NE	10 56	35.5		24 48	43	(12937)	(37)	(16.0)					
10	Mrk 238	12 59	20.7		65 16	06		14816	171	15.92	0.8 0.7			14.8
11	IRAS 13001-2339	13 00	10.5		-23 39	13		6417	130	14.68	1.3 0.5	I0:p		6.5
12	NGC 5256A	13 36	14.5		48 31	47		8316	55	(14.1)	0.5 0.4	Comp.p	Sy2	9.5
	NGC 5256B	13 36	15.0		48 31	54		8419	48	13.67	0.7 0.6	Comp.p	L	
13	Mrk 463	13 53	39.6		18 36	57	(15289)		(17.75)				Sy2	3.9
		13 53	39.8		18 36	58	(14990)		(17.25)				Sy1	
14	IC 4395	14 15	06.2		27 05	18		10947	7	14.84	1.1 0.8	S?	H II	6.0
15	UGC 9618A	14 54	47.9		24 48	28		10029	10	15.30	0.8 0.7	Sc		41.6
	UGC 9618B	14 54	48.2		24 49	03		10157	53	15.70	0.8 0.3	Sb	H II/L	
16	Mrk 848	15 16	19.5		42 55	30		12049	131	15.95	0.7 0.3			6.5
17	NGC 6090	16 10	24.1		52 35	00	(9062)	(30)	(15.0)	(0.3 0.3)		Sd p	H II	6.5
		16 10	24.6		52 35	04	(8822)	(30)	(14.5)	(0.4 0.2)		Sd p	H II	
18	IRAS 20010-2352	20 01	04.2		-23 52	25		15194	69	17.07	0.4 0.3		Sy2	8.9
19	II Zw 96	20 55	04.6		16 56	07	(10630)	(81)	(16.41)				H II	11.0
		20 55	05.0		16 55	58	(10770)	(81)	(15.20)					

Note: the values in brackets are from the NED database, all others are weighted means from the LEDA database.

flux density in mJy we used the calibration procedure described in Matthews et al. (2001), see also Matthews et al. (1998) and Matthews & van Driel (2000). This procedure yields an internal calibration accuracy of about  $\pm 15\%$  near the rest frequency of the 21cm line, and  $\pm 25\%$  for the highest redshift source in the sample, at  $V=24,000$   $\text{km s}^{-1}$  (1300 MHz), as less standard calibration observations were made at these infrequently observed high velocities.

Another consequence of observing redshifted objects down to a frequency of 1300 MHz, far outside the protected 1400-1427 MHz frequency band allocated on a primary base to the Radio Astronomy Service (e.g., CRAF Handbook on Radio Astronomy 1997), is the occurrence of strong radio interference (RFI) signals, which were especially noticeable in the 10,000–12,000  $\text{km s}^{-1}$  range (see, e.g., the remarks on Mrk 848 in Sect. 4.1).

### 3.2. Arecibo observations

During an observing run at Arecibo from 1 to 13 november, 2000, we obtained HI spectra of the 4 sample galaxies which could be observed within the declination range of the 305-m diameter telescope and the allocated sidereal time slots: IRAS 03359+1523, 04232+1436, 10565+2448 and II Zw 96. Data were taken with the  $L$ -narrow receiver, set to linear polarisation, with two polarisations, 4096 channel subcorrelators and nine channel sampling. Each subcorrelator had a 12.5 MHz bandpass, resulting in a 1.3  $\text{km s}^{-1}$  resolution. Observations were taken in 3 minute ON/OFF pairs, followed by a 10 sec ON/OFF calibration pair. The data were reduced using the ANALYZ software package (Deich 1990). The two polarisations were combined, and corrections were applied for the variations in the gain and system temperature of the telescope with zenith angle. A 21-channel boxcar velocity smoothing was applied, resulting in a resolution of 27.0  $\text{km s}^{-1}$ . Baselines were then fitted to the data using the GALPAK package

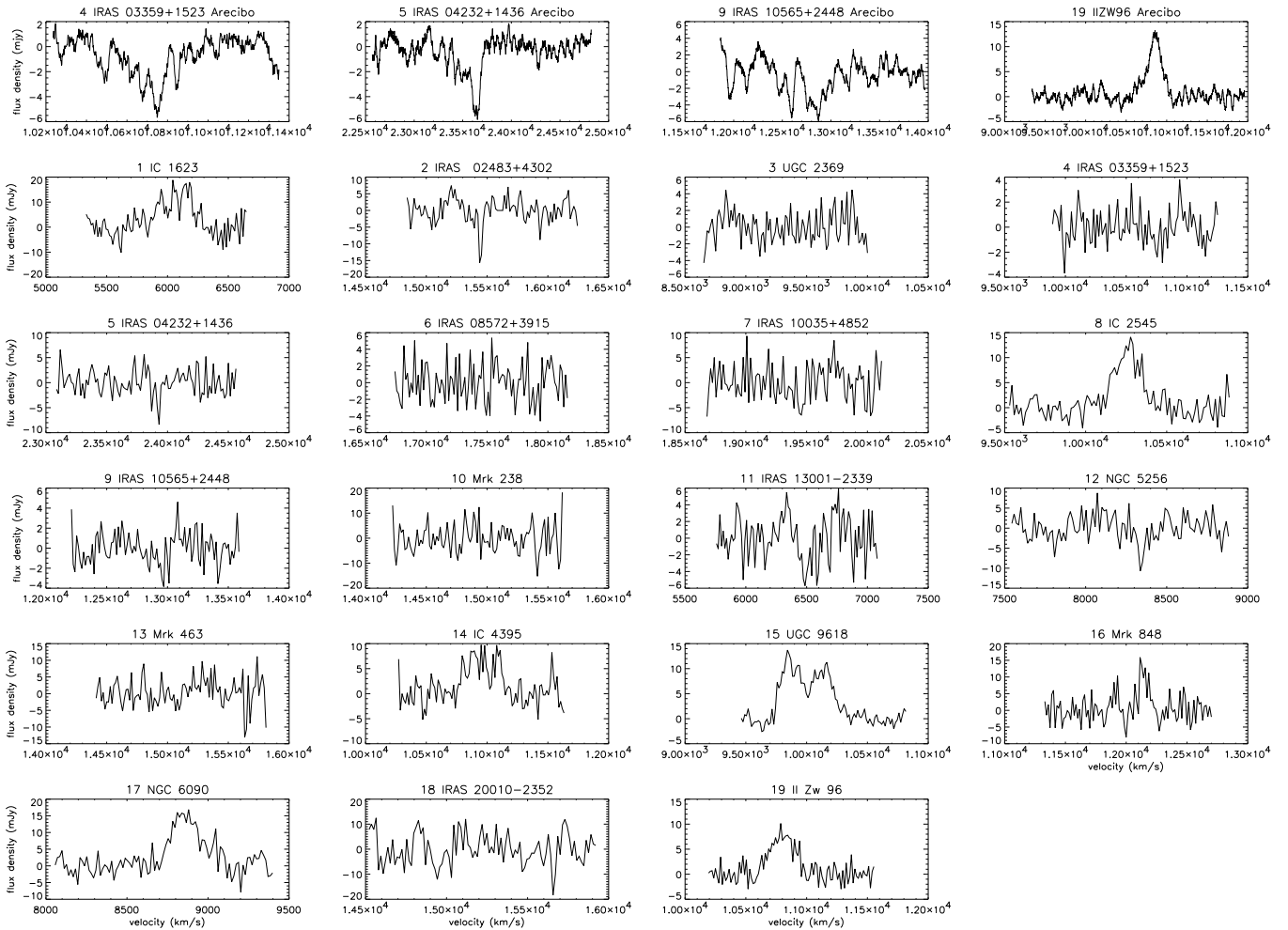


**Fig. 2.** Arecibo (top row) and Nançay 21-cm H I line spectra. Velocity resolution is  $27.0 \text{ km s}^{-1}$  for the 4 Arecibo profiles and  $15.8 \text{ km s}^{-1}$  for the 19 Nançay spectra, radial heliocentric velocities are according to the optical convention. The spectra are shown in the same order as in Fig. 1 and Table 1. The line signal in the Nançay Mrk 848 spectrum is caused by residual radio interference, see Sect. 4.

adapted by K. O’Neil, which was also used to correct the velocities to the heliocentric system and to determine the global H I line parameters.

#### 4. Results and Discussion

The 19 Nançay and the 4 Arecibo H I spectra are shown in Fig. 2. Raw, measured radial velocities,  $V_{HI}$  (in the optical convention) and their uncertainties, integrated line fluxes,  $I_{HI}$ , velocity widths at 50% and 20% of peak maximum,  $W_{50}$  and  $W_{20}$ , and rms noise levels of our spectra were determined using the SIR data reduction package for the Nançay data and the adapted GALPAK package for the Arecibo data (see Matthews et al. 2001, and references therein).

No corrections have been applied to these values for, e.g., instrumental resolution or cosmological stretching (e.g., Matthews et al. 2001). We estimated the uncertain-

ties,  $\sigma_{V_{HI}}$ , in the central H I velocities following Fouqué et al. (1990):

$$\sigma_{V_{HI}} = 4R^{0.5}P_W^{0.5}X^{-1} [km/s] \quad (1)$$

where  $R$  is the instrumental resolution in  $\text{km s}^{-1}$ ,  $P_W = (W_{20} - W_{50})/2$  [km/s] and  $X$  is the signal-to-noise ratio of a spectrum, which we defined as the ratio of the peak flux density and the rms noise. According to Fouqué et al., the uncertainty in the linewidths is  $2\sigma_{V_{HI}}$  for  $W_{50}$  and  $3\sigma_{V_{HI}}$  for  $W_{20}$ . These H I profile parameters are listed in Table 2, together with values found in the literature. For non-detections, the estimated upper limits to the integrated H I fluxes are  $2\sigma$  values for flat-topped profiles with a linewidth equal to those measured for the CO line emission of the objects, either FWHM or half of FWZI values (see Table 3, for the CO data references see Gao & Solomon 1999). Derived global properties of the 19 sam-

**Table 2.** Basic HI data - new results and literature values

No.	Ident	R.A.		Dec	rms	$I_{HI}$	$V_{HI}$	$W_{50}$	$W_{20}$	Tel	Ref
		(1950.0)									
		hh mm ss.s	dd mm ss	mJy	Jy km s <sup>-1</sup>	km s <sup>-1</sup>	km s <sup>-1</sup>	km s <sup>-1</sup>			
1	IC 1623	01 05 21.0	-17 46 23	5.51	4.56	6053±20	287	331	N	*	
					3.30	6078	244	380	N	Ma91	
2	IRAS 02483+4302	02 48 19.8	43 02 53	4.90	<2.45				N	*	
3	UGC 2369	02 51 15.8	14 46 14	2.43	<2.19				N	*	
4	IRAS 03359+1523	03 35 57.9	15 23 11	1.76	0.48	9761	229:	—	A	Ha97	
					<i>abs.</i>	<i>9406</i>	—	274	A	MS88	
					<0.83				N	*	
5	IRAS 04232+1436	04 23 15.2	14 36 53	3.43	<i>abs.</i>	<i>10725</i>	<i>189</i>	—	A	*	
					<2.74	<i>10717</i>	—	294	A	MS88	
					0.59				N	*	
6	IRAS 08572+3915	08 57 12.9	39 15 39	3.11	<1.68				A	*	
7	IRAS 10035+4852	10 03 35.7	48 52 23	4.85	<2.43				N	*	
8	IC 2545	10 03 52.3	-33 38 24	3.25	2.56	10257±16	182	228	N	*	
9	IRAS 10565+2448	10 56 36.2	24 48 40	2.13	<1.28				N	*	
					1.17	<i>abs</i>	<i>12825:</i>	—	—	A	*
					>0.11	13100	—	>137	A	MS88	
10	Mrk 238	12 59 20.7	65 16 06	7.74	<5.42				A	MS88	
11	IRAS 13001-2339	13 00 10.5	-23 39 13	3.43	<3.09				N	*	
12	NGC 5256	13 36 15.0	48 31 51	4.39	<2.51				N	*	
13	Mrk 463	13 53 39.7	18 36 57	5.93	<3.55				N	*	
					0.20	15230	—	200	A	Hu87	
					≤0.24				A	BB83	
14	IC 4395	14 15 06.2	27 05 18	3.26	6.0	14702			G	He78	
					2.54	10954±18	308	340	N	*	
					1.30	10949	285	328	N	Ma91	
15	UGC 9618	14 54 48.3	24 48 42	1.42	0.62:	10946:	199:	—	A	Fr88	
					5.43	9980±11	419	529	N	*	
					3.86	10029	317	442	N	Ma91	
16	Mrk 848	15 16 19.5	42 55 30	4.77	>4.66	9982	—	513	A	MS88	
					<i>abs.</i>	<i>9990</i>	—	215	A	MS88	
					—				N	*	
17	NGC 6090	16 10 24.0	52 35 04	3.57	4.30	8901±28	203	357	N	*	
					3.21	8841	211	232	N	Ma91	
					3.4	8871	—	348	G	HR89	
18	IRAS 20010-2352	20 01 04.2	-23 52 25	8.35	5.29	8873	—	—	G	Bu87	
					<9.19				N	*	
					2.26	10803±17	270	315	N	*	
19	II Zw 96	20 55 04.8	16 56 02	2.15	2.55	10860±9	189	412	A	*	
					1.16				A	MS88	
					2.34	10822	211	320	A	GH93	
					>2.08	10810	—	263	A	MS88	
					<i>abs.</i>	<i>11132</i>	—	300	A	MS88	

Notes: ‘:’ denotes an uncertain value; values in *italics* are for absorption line profiles; upper limits to  $I_{HI}$  are  $2\sigma$  values for flat-topped profiles with linewidths assumed equal to the CO line values (see Table 3).

HI references and telescope codes:

BB83	Biegling & Biermann (1983)	Bu87	Bushouse (1987)
Fr88	Freudling et al. (1988)	GH93	Giovanelli & Haynes (1993)
Ha97	Haynes et al. (1997)	He78	Heckman et al. (1978)
HR89	Huchtmeier & Richter (1989)	Hu87	Hutchings et al. (1987)
Ma91	Martin et al. (1991)	MS88	Mirabel & Sanders (1988)
*	present paper		

A Arecibo                      N Nançay                      G Green Bank 90m

ple galaxies are listed in Table 3; the CO line luminosity values are from Gao & Solomon (1999).

Of these 19 luminous infrared mergers, 10 were observed here for the first time in the 21cm line (IC 2545; IRAS 02483+4302, 04232+1436, 08572+3915, 10035+4852, 13001-2339 and 20010-2352; Mrk 238 and 848; NGC 5256 - i.e., Nos. 2, 5, 6, 7, 8, 10, 11, 12, 16 and 18). For the 9 objects observed previously, our observations served to obtain new, independent HI profile parameters, as in many cases there were discrepancies be-

tween published data (see Table 2 and Sect. 4.1). Of the 6 objects in which we clearly detected line emission (II Zw 96; IC 1623, 2545 and 4395; UGC 9618; NGC 6090 - i.e., Nos. 1, 8, 14, 15, 17 and 19), one (IC 2545, No. 8) had not been detected before. The HI fluxes measured previously at Nançay by Martin et al. (1991) for 4 of these 6 objects are on average about 50% lower; we prefer to use our Nançay flux values, as they are based on recent external calibrations (see Sect. 3).

In all, 8 of the 19 galaxies observed have reliable HI emission line detections: the abovementioned 6 we detected, as well as Mrk 463 and UGC 2369 (i.e., Nos. 3 and 13). Two others show an HI line in absorption: IRAS 03359+1523 and 10565+2448 (Nos. 4 and 9), and for one (Mrk 848, no. 16) no conclusion could be drawn due to strong interference. Global HI profile parameters of (merging) galaxies can depend on the telescope used, though, as the different beam sizes (ranging from 3'6 diameter at Arecibo to 12' for the Green Bank 90m) may include extended gas structures, like tails (e.g., Hibbard & Yun 1999a), or nearby, confusing galaxies. And even observations made with the same instruments may, surprisingly enough, sometimes show significantly different profiles (e.g., for UGC 2369 and II Zw 96). See the notes on individual objects in Sect. 4.1. for details.

The derived HI masses listed in Table 3 are plotted as function of the projected linear separation between the two merger components in Figure 3. Concerning the adopted total HI masses for galaxies with more than one spectrum available: for the 5 galaxies detected by us we used our Nançay results, except for II Zw 96, where we used the average of all 3 available emission line fluxes; for UGC 2369, we used the Arecibo detection by Haynes et al. (1997) and for Mrk 463 we used the Arecibo detection by Hutchings et al. (1987) – see also Sect. 4.1.

Six out of the 9 detected objects have a  $\log(M_{HI})$  exceeding 9.8, while 2 (UGC 2369 and Mrk 463 - i.e., Nos 3 and 13) have values  $\sim 9.3$ . A similar plot for the  $H_2$  masses as function of projected separation, showing a clear correlation, can be found in Gao & Salomon (1999). The relation between the HI mass and separation will be examined further in Gao et al. (in preparation), using all available HI line data, both published and others, for a sample of about 30 objects.

#### 4.1. Notes to individual galaxies

We searched the vicinity of the target objects for nearby spiral galaxies which could possibly give rise to confusion in those Nançay HI profiles where line emission was detected. We used the online NED and LEDA databases (see Webpages <http://nedwww.ipac.caltech.edu> and <http://leda.univ-lyon1.fr/pages-html/single.html>, respectively), in an area of  $5.5 \times 30'$  ( $\alpha \times \delta$ ) round the pointing centre, i.e. about 1.5 times the HPBW, as well as optical images extracted from the Digitized Sky Survey (see Fig. 1). For quoted NED values the original literature reference is given here (in brackets), while the LEDA data listed are weighted average values.

**1. IC 1623** Just inside the Nançay search area, but outside the area shown in Fig. 1, lies Sb spiral IC 1622 at an E-W separation of 2'5, i.e. 1.4 times the E-W HPBW, SW of the center of the IC1623A/B pair; its  $V_{opt}=6343 \pm 60 \text{ km s}^{-1}$ , i.e.  $285 \text{ km s}^{-1}$  higher than the mean optical velocity of the pair, it has magnitude

$B_T=14.53$ , diameter  $D_{25}=0'7$  and an axial ratio of 0.78. Seen the separation in the sky and in velocity, we do not expect our Nançay spectrum to be contaminated by this galaxy, unless it has an exceptionally large HI envelope. Another nearby companion galaxy, nearly 5' NE of IC 1623 at only an E-W separation of 1'5, was detected in the VLA HI maps (for preliminary results, see Hibbard & Yun 1996; also for detailed maps, check <http://www.cv.nrao.edu/~jhibbard/vv114/>), which can only contribute less than 10% of our Nançay detected HI emission. Our Nançay data showed strong baseline curvature in the  $H$  polarisation only, and we therefore used the unaffected  $V$  polarisation data for the data reduction.

**2. IRAS 02483+4302** In the LEDA database, only a single object (PGC 90441) is listed, while two are listed in the NED database: Anon 0248+43A, a 16.52 mag object at  $V=15576 \pm 46 \text{ km s}^{-1}$  (Strauss et al. 1992), and Anon 0248+43B, a 17.36 mag object at  $V=15199 \text{ km s}^{-1}$ . We used the LEDA entries for PGC 90441 for Table 1. Our Nançay data showed stronger baseline curvature in the  $V$  polarisation, where we therefore fitted a 5<sup>th</sup> order polynomial to the data. The data were affected by strong, narrow radio interference in both  $H$  and  $V$  polarisation around  $15,525 \text{ km s}^{-1}$ ; this strong, spurious signal has been blanked out in Figure 1. At full velocity resolution, the narrow absorption feature seen at  $15,365 \text{ km s}^{-1}$  seems to be due to weaker interference, as it is much too narrow to be an absorption feature originating in the merger galaxy.

**3. UGC 2369** Within the Arecibo beam (3'6 HPBW) an HI absorption line profile (minimum flux density  $\sim 3 \text{ mJy}$ ) was reported centered at  $V=9406 \text{ km s}^{-1}$  with a  $W_{20}$  width of  $274 \text{ km s}^{-1}$  by Mirabel & Sanders (1988), while an emission line (of average flux density  $\sim 2 \text{ mJy}$ ) was reported at  $V=9761 \text{ km s}^{-1}$  with a  $W_{50}$  width of  $229 \text{ km s}^{-1}$  by Haynes et al. (1997), who note that the measured width of their profile is poor. The mean optical velocities of the 2 galaxies are  $9463 \pm 152$  and  $9380 \pm 118 \text{ km s}^{-1}$  (LEDA), respectively, corresponding very well to the velocity of the reported absorption line, but not incompatible with the reported emission line velocity either, given the uncertainties in the optical velocities. No line signal was noted in our Nançay spectrum, with an rms of  $2.4 \text{ mJy}$ . Mirabel & Sanders measured a 21 cm continuum flux density of  $56 \text{ mJy}$ . For the total HI mass, we used the Arecibo detection by Haynes et al. (1997), which may be a lower limit, however, given the broad CO linewidth ( $FWZI \sim 900 \text{ km s}^{-1}$ , Gao & Solomon (1999)) and possible HI absorption at lower velocity.

**4. IRAS 03359+1523** In our Nançay spectrum, with an rms of  $1.7 \text{ mJy}$ , no line signal was noted, neither in emission nor in absorption. Within the Arecibo beam (3'6 HPBW) an HI absorption line profile (minimum flux density  $\sim 5 \text{ mJy}$ ) was detected by Mirabel & Sanders (1988) and in the present survey. The mean velocity of the absorption feature,  $10721 \text{ km s}^{-1}$ , is  $95 \text{ km s}^{-1}$  higher than

**Table 3.** Global properties of the sample galaxies

		$d_L$ Mpc	Sep kpc	$L_{IR}$ $10^{11}L_\odot$	$L_{CO}$ $10^9L_l$	$\log M_{HI}$ $M_\odot$	assumed linewidth $\text{km s}^{-1}$
1	IC 1623	81.7	6.1	4.7	10.7	9.86	
2	IRAS 02483+4302	213.6	3.6	6.2	2.9	<10.42	250
3	UGC 2369	127.8	13.1	3.9	7.2	9.27	
4	IRAS 03359+1523	144.5	6.5	3.3	6.9	<i>abs.</i>	235
5	IRAS 04232+1436	327.1	6.3	11.1	9.0	<10.08	400
6	IRAS 08572+3915	236.8	4.6	11.9	1.7	<10.35	270
7	IRAS 10035+4852	263.3	9.8	9.3	7.0	<10.60	250
8	IC 2545	137.6	3.1	4.5	2.9	10.06	
9	IRAS 10565+2448	174.2	6.2	9.6	5.8	<i>abs.</i>	
10	Mrk 238	204.0	13.2	2.5	6.8	<10.73	350
11	IRAS 13001-2339	86.4	2.6	2.4	2.6	<9.73	450
12	NGC 5256	110.6	4.8	3.1	5.7	<9.86	400
13	Mrk 463	204.4	3.5	5.3	2.8	9.29	
14	IC 4395	147.9	4.0	2.2	4.0	10.12	
15	UGC 9618	137.0	25.8	4.1	17.0	10.38	
16	Mrk 848	162.2	4.8	7.2	7.0	—	300
17	NGC 6090	117.6	3.5	3.0	5.0	10.15	
18	IRAS 20010-2352	206.4	8.1	4.7	6.4	<10.96	550
19	II Zw 96	149.9	7.4	6.6	6.0	10.09	

Notes: upper limits to  $\log M_{HI}$  are  $2\sigma$  values for flat-topped profiles with assumed linewidths equal to the measured CO line values; *abs* denotes absorption line spectra;  $L_l$  is in units of  $\text{K km s}^{-1} \text{pc}^{-2}$

the optical systemic velocity, which has an uncertainty of  $45 \text{ km s}^{-1}$ . Mirabel & Sanders measured a 21 cm continuum flux density of 27 mJy.

**5. IRAS 04232+1436** Both our Nançay and Arecibo spectra show a quite narrow absorption line (FWHM=90  $\text{km s}^{-1}$  at Arecibo, centered at  $V=23567 \text{ km s}^{-1}$ ), reaching a minimum flux density of about 5 to 6 mJy. These are likely due to interference, however, as the mean velocities of these features are about  $270 \text{ km s}^{-1}$  different, and the measurements were made at 1308 MHz, far outside the protected 1400-1427 MHz band. The Arecibo spectrum also shows a broader ( $W_{20}=290 \text{ km s}^{-1}$ ) absorption feature at the -2 mJy level, too faint for clear detection in Nançay, which may also be due to interference. In conclusion, the data do not provide sufficient evidence for the detection of an HI line.

**6. IRAS 08572+3915** In the LEDA database, only a single object (PGC 25295) is listed, while two are listed in the NED database (IRAS 08572+3915NW and SE), based on near-infrared imaging observations (Zhou et al. 1993); as positions only are given for these two components in NED, we have used the LEDA entries for Table 1.

**7. IRAS 10035+4852** Very close, interacting galaxy pair. In the LEDA database, only a single object (PGC 29385) is listed, while two are listed in the NED database: the E and W objects has optical redshifts of, respectively,

$19371\pm 42$  and  $19421\pm 53 \text{ km s}^{-1}$  (Strauss et al. 1992). We have used the LEDA entries for Table 1.

**8. IC 2545** Very close, interacting galaxy pair. In the LEDA database, only a single object (PGC 29334) is listed, while two are listed in the NED database, based on Lauberts & Valentijn (1989). Besides positions, for the NW object a radial velocity ( $10267\pm 86 \text{ km s}^{-1}$ ) and a B magnitude (15.27) are listed, and for the SE object only a B magnitude (16.83). We have used the LEDA entries for Table 1. Detected for the first time in HI.

**9. IRAS 10565+2448** Two distinct, interacting galaxies can be seen on the Digital Sky Survey. In the LEDA database, only a single object (PGC 33083) is listed, while two are listed in the NED database; we used the latter for Table 1. The optical redshift references are Kim et al. (1995) for the W object and Strauss et al. (1992) for the NE object. Within the Arecibo beam (3'6 HPBW) an HI line profile showing both emission and much stronger absorption (maximum/minimum flux density  $\sim +1/-5 \text{ mJy}$ , respectively) was reported by Mirabel & Sanders (1988) - see the two entries in Table 2, where the emission line values are lower limits - who measured a 21 cm continuum flux density of 44 mJy. Our Arecibo observations show some structure in the base line, as they were taken after sunrise. The deepest and broadest negative feature in our data corresponds well to the one noted by Mirabel & Sanders. We lack the sensitivity, however, to



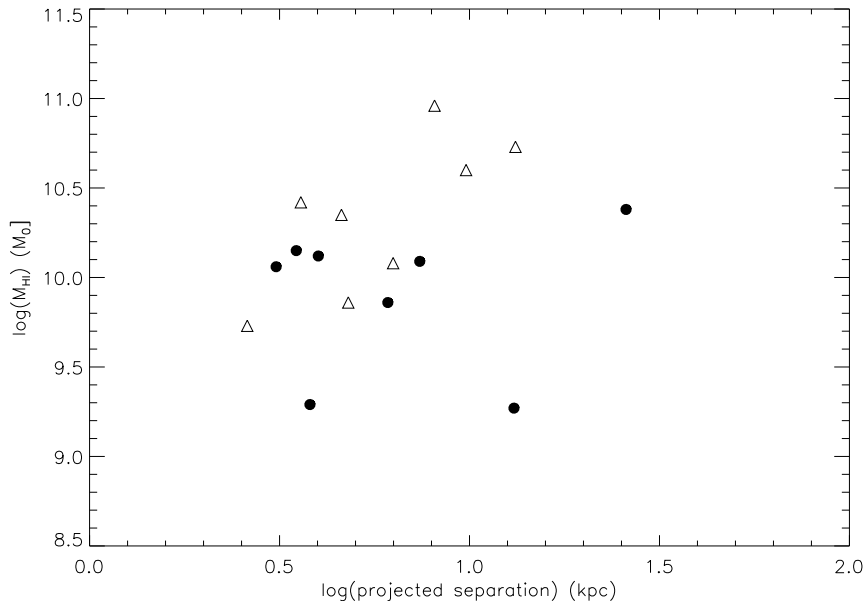


**Fig. 3.** Total H I gas mass plotted as function of the projected linear separation between the two components of the 16 mergers observed which show line emission or for which an upper limit to the line flux could be estimated; objects which show an absorption line only were excluded. Filled circles denote detections and triangles upper limits. Upper limits to the H I masses are  $2\sigma$  values for flat-topped profiles with assumed widths equal to the measured CO line width of the objects (see Table 3).

verify their extremely faint ( $\sim 0.5$  mJy), very broad absorption feature extending down to about  $12,300 \text{ km s}^{-1}$ . We see no sign of their emission feature adjacent (at higher velocity) to the deeper absorption line.

**11. IRAS 13001-2339 = ESO 507-G070** Our Nançay data, obtained over 12 days, showed baseline curvature in both  $H$  and  $V$  polarisation, and we therefore fitted a  $5^{\text{th}}$  order polynomial to the data.

**12. NGC 5256** Both the LEDA and NED databases have entries for 2 objects. In the LEDA database, a B magnitude is given for one object only (13.67), while in NED the same B magnitude (14.1) given for both objects.

**13. Mrk 463** The Arecibo detection of Mrk 463 (Hutchings et al. 1987) at  $0.2 \text{ Jy km s}^{-1}$  is at the  $4\sigma$  level, with a peak flux density of  $1.6 \text{ mJy}$ ; the authors note that the profile was detected in both observing runs. Heckman et al. (1978) note that their Green Bank flux measurement is relatively uncertain,  $6.0 \pm 2.3 \text{ Jy km s}^{-1}$ , and that it would imply a very high  $M_{\text{HI}}/L_B$  ratio for Mrk 463 if all gas detected resides in this galaxy. The reported Green Bank flux is 30 times higher than the Arecibo value, and the central velocities of these detections seem incompatible:  $14702$  and  $15230 \text{ km s}^{-1}$ , respectively ( $\Delta V = 528 \text{ km s}^{-1}$ ), for a  $W_{20}$  profile width of  $200 \text{ km s}^{-1}$  measured at Arecibo. Inside the Green Bank HPBW but well outside the Arecibo beam, the DSS shows only one other galaxy that might be a source of confusion in the Green Bank

H I spectrum: CGCG 103-016,  $6'1$  to the SE of the target galaxy, a  $B_T$  15.5 object of  $0.4$  diameter and unknown redshift. If it were the sole source of H I emission within the Green Bank beam, it would have an  $M_{\text{HI}}/L_B$  ratio of  $1.4 M_{\odot}/L_{\odot,B}$ , which is about 4 times the mean ratio for an Sc spiral (Roberts & Haynes 1994), but not unheard of for late-type galaxies. The morphology of CGCG 103-016 is hard to discern, however, as a relatively bright star is situated close to its centre. In conclusion, CGCG 103-016 may be the cause of the discrepant Green Bank flux. For the total H I mass, we used the Arecibo detection by Hutchings et al. (1987).

**14. IC 4395** Freudling et al. (1988) note that the parameters of their Arecibo H I profile are uncertain, as it was detected at the edge of the band. Considerable flux may well have been missed within the Arecibo band, given the fact that our Nançay integrated line flux is considerably (factor 4) larger than the Arecibo flux and that our  $W_{50}$  linewidth of  $308 \text{ km s}^{-1}$  is 1.5 times larger than the Arecibo value. Our Nançay data showed strong baseline curvature in the  $V$  polarisation, and we therefore used only the unaffected  $H$  polarisation data for the data reduction.

**15. UGC 9618** All three available spectra (one from Arecibo and 2 from Nançay, see Table 2) show a clear emission line with a pronounced central depression. Only for the Arecibo spectrum, Mirabel & Sanders (1988) interpreted this as an absorption feature, see their two entries

in Table 2; they report a 21 cm continuum flux density of 109 mJy.

**16. Mrk 848** The Nançay data were heavily affected by radio interference, particularly in the  $H$  but also in the  $V$  polarisation, within the range where the HI line emission was expected. Though we used only the least affected data for the spectrum shown in Fig. 2, the remaining emission features appear to be due to RFI. We therefore do not consider this galaxy as detected in our survey, but we cannot give a proper upper limit to its integrated line flux, due to the remnant RFI occurring at its redshift.

**17. NGC 6090** In the LEDA database, only a single object (PGC 57437) is listed, while two are listed in the NED database. We used the NED entries for Table 1; both optical redshifts are from Kim et al. (1995).

**19. II Zw 96** In the LEDA database, only a single object (PGC 65779) is listed, while four are listed in the NED database; we used the NED entries of the first two for Table 1. Near-infrared imaging (Goldader et al. 1997) revealed 4 sources; one (1<sup>st</sup> in Table 1) seems to be a relatively quiescent spiral galaxy, another (2<sup>nd</sup> in Table 1) may be a galaxy nucleus, since it shows hints of a bar as well as powerful starburst activity, and the other two are most likely highly obscured, luminous starburst regions. Huge molecular gas concentrations were discovered recently around these two highly obscured starburst regions by Gao et al. (2000a). All published Arecibo, Green Bank and Nançay spectra show a clear emission feature. Only Mirabel & Sanders (1988) reported an absorption feature (minimum flux density -2.5 mJy) in their Arecibo profile, adjacent to the emission line (see Table 2), which does not occur in the Arecibo spectra taken by us or by Giovanelli & Haynes (1993); we therefore consider it to be spurious.

*Acknowledgements.* We would like to thank Drs. K. O’Neil and T. Ghosh for their help with the Arecibo observations and data reduction and Ms. M. Gendre for her help with the Nançay data reduction. We have made use of the NASA/IPAC Extragalactic Database (NED) which is operated by the Jet Propulsion Laboratory, California Institute of Technology, under contract with the U.S. National Aeronautics and Space Administration, as well as the Lyon-Meudon Extragalactic Database (LEDA) supplied by the LEDA team at the CRAL-Observatoire de Lyon (France). The Unité Scientifique Nançay of the Observatoire de Paris is associated as Unité de Service et de Recherche USR No. B704 to the French Centre National de Recherche Scientifique (CNRS). Nançay also gratefully acknowledges the financial support of the Département du Cher, the European Community, the FNADT and the Région Centre.

## References

- Bieging, J. H., & Biermann, P. 1983, A&A, 88, 161  
 Bushouse, H. A. 1987, ApJ, 320, 49  
 Bushouse, H. A., Werner, M. W., & Lamb, S. A. 1988, ApJ, 335, 74  
 Combes, F., Prugniel, P., Rampazzo, R., & Sulentic, J. W. 1994, A&A, 281, 725  
 Condon, J. J., Huang, Z.-P., Yin Q. F., & Thuan, T. X. 1991, ApJ, 378, 65  
 Deich, W. 1990, ANALYZ User’s Guide (Arecibo Observatory)  
 Downes, D., & Solomon, P. M. 1998, ApJ, 507, 615.  
 Fouqué, P., Bottinelli, L., Durand, N., Gouguenheim, L., & Paturel, G. 1990, A&AS, 86, 473  
 Freudling, W., Haynes, M. P., & Giovanelli, R. 1988, AJ, 96, 1791  
 Gao, Y. 1996, Ph.D. thesis, State University of New York at Stony Brook  
 Gao, Y., Gruendl, R., Lo, K. Y., Hwang, C. Y., & Veilleux, S. 1997, in Star Formation: Near and Far, ed. S. S. Holt, & L.G. Mundy (AIP Press: New York), 319  
 Gao, Y., & Solomon, P. M. 1999, ApJ, 512, L99  
 Gao, Y., Gruendl, R. A., Hwang, C. Y., Lo, K. Y. 1999, in Galaxy Interactions at Low and High Redshift, IAU Symposium 186, ed. J. Barnes, & D. Sanders (Dordrecht: Kluwer), 227  
 Gao, Y., & Solomon, P. M. 2000a, ApJ, submitted  
 Gao, Y., & Solomon, P. M. 2000b, ApJ, submitted  
 Gao, Y., Goldader, J. D., Seaquist, E. R., & Xu, C. 2000a, in Science with the Atacama Large Millimeter Array (ALMA), ed. A. Wootten, in press (astro-ph/0008114)  
 Gao, Y., Lo, K. Y., Lee, S.-W., & Lee, T.-H. 2000b, ApJ, in press (astro-ph/0010128)  
 Garwood, R. W., Dickey, J. M., & Helou, G. 1987, ApJ, 322, 88  
 Genzel, R., Lutz, D., Sturm, E., et al. 1998, ApJ, 498, 569  
 Giovanelli, R., & Haynes, M. P. 1993, AJ, 105, 1271  
 Goldader, J. D., Goldader, D. L., Joseph, R. D., Doyon, R., & Sanders, D. B. 1997, AJ, 113, 1569  
 Haynes, M.P., Giovanelli, R., Herter, T., et al. 1997, AJ, 113, 1197  
 Heckman, T. M., Balick, B., & Sullivan, W. T. 1978, ApJ, 224, 745  
 Hibbard, J. E., & van Gorkom, J. H. 1996, AJ, 111, 655  
 Hibbard, J. E., & Yun, M. S. 1996, in Cold Gas at High Redshift, ed. M. Bremer et al. (Dordrecht: Kluwer), 47  
 Hibbard, J. E., & Yun, M. S. 1999a, AJ, 118, 162  
 Hibbard, J. E., & Yun, M. S. 1999b, ApJ, 522, 93  
 Huchtmeier, W. A., & Richter, O.-G. 1989, A General Catalog of HI Observations of Galaxies (Springer: Heidelberg)  
 Hutchings, J. B., Gower, A. C., & Price, R. 1987, AJ, 93, 6  
 Jackson, J.M., Snell, R. L., Ho, P. T. P., & Barrett, A. H. 1989, ApJ, 337, 680  
 Kennicutt, R. C., Roettiger, K. A., Keel, W. C., van der Hulst, J. M., & Hummel, E., 1987, AJ, 93, 1011  
 Kennicutt, R. C. 1998, ApJ, 498, 541  
 Kim, D.-C., Sanders, D. B., Veilleux, S., Mazzarella, J. M., & Soifer, B. T. 1995, ApJS, 98, 129  
 Lauberts, A., & Valentijn, E. A. 1989, The Surface Photometry Catalogue of the ESO-Uppsala galaxies (ESO: Garching bei München)  
 Leech, K. J., Rowan-Robinson, M., Lawrence, A., & Hughes, J. D. 1994, MNRAS 267, 253  
 Lo, K. Y., Gao, Y., & Gruendl, R. 1997, ApJ, 475, L103.  
 Martin, J. M., Bottinelli, L., & Gouguenheim, L. 1991, A&A, 245, 393  
 Matthews, L. D., van Driel, W., & Gallagher, J. S. 1998, AJ, 116, 1196

- Matthews, L. D., & van Driel, W. 2000, *A&AS*, 143, 421
- Matthews, L. D., van Driel, W., & Monnier-Ragaine, D. 2001, *A&AS*, in press (astro-ph/0010075)
- Mirabel I. F., & Sanders, D. B. 1988, *ApJ*, 335, 104
- Mirabel I. F., & Sanders, D. B. 1989, *ApJ*, 340, L53
- Mirabel I. F. 1997, private communication
- Murphy, T. W., Armus, L., Matthews, K., et al. 1996, *AJ*, 111, 1025
- Roberts, M. S., & Haynes, M. P. 1994, *ARA&A*, 32, 115
- Sanders, D. B., Soifer, B. T., Elias, J. H., et al. 1988, *ApJ*, 325, 74
- Sanders, D. B. 1992, in *ASP Conf. Ser. 31, Relationships between Active Galactic Nuclei and Starburst Galaxies*, ed. A. Filippenko, 303
- Sanders, D. B., & Mirabel I. F. 1996, *ARA&A*, 34, 749
- Sanders, D. B. 1999, *Ap&SS* 266, 331
- Scoville, N. Z., Sargent, A. I., Sanders, D. B., & Soifer, B. T. 1991, *ApJ*, 366, L5
- Scoville, N. Z., Evans, A. S., Thompson, R., et al. 2000, *AJ*, 119, 991
- Smith, H. E., Lonsdale, C. J., & Lonsdale, C. J. 1998, *ApJ*, 492, 137
- Soifer, B. T., Neugebauer, G., Matthews, K., et al. 2000, *AJ*, 119, 509
- Solomon, P. M., Downes, D., & Radford, S. J. E. 1992, *ApJ*, 387, L55
- Solomon, P. M., Downes, D., Radford, S. J. E., & Barrett, J. 1997, *ApJ*, 478, 144
- Strauss, M. A., Huchra, J. P., Davis, M., et al. 1992, *ApJS*, 83, 29
- Toomre, A., & Toomre, J. 1972, *ApJ*, 178, 623.
- Toomre, A. 1977, in *The Evolution of Galaxies and Stellar Populations*, ed. B.M. Tinsley B.M., & R.B. Larson (New Haven: Yale Univ.), 401
- van den Broek, A. C., van Driel, W., de Jong, T., et al. 1991, *A&AS*, 91, 61
- Veilleux, S., Sanders, D. B., & Kim, D.-C. 1997, *ApJ*, 484, 92
- Veilleux, S., Sanders, D. B., & Kim, D.-C. 1999, *ApJ*, 522, 139
- Young, J. S., Schloerb, F. P., Kenney, J. D., & Lord, S. D. 1986, *ApJ*, 304, 443
- Zhou, S., Wynn-Williams, C. G., & Sanders, D. B. 1993, *ApJ*, 409, 149